Advances in Concrete Construction, *Vol. 15, No. 3 (2023) 149-159*
https://doi.org/10.12989/acc.2023.15.3.149

Effect of activator types on cement mortar with polymeric aluminum chloride waste residue

Ping Xu*[1], Yuhao Cui [1b], Dong Han [2], Minxia Zhang [1c] and Yahong Ding [1d]

[1] *College of Civil Engineering, Henan Polytechnic Univ., Jiaozuo, Henan 454003, China*
[2] *Citic Heavy Industry Engineering Technology Co. LTD, Luoyang City, Henan 471000, China*

(*Received August 24, 2022, Revised January 28, 2023, Accepted February 21, 2023*)

Abstract. Water glass (WG) and sodium sulfate (SS) were used to prepare polymeric aluminum chloride residue cement mortar (PACRM) by single and compound blending with polymeric aluminum chloride waste residue, respectively. The structural strength and textural characteristics examinations showed that PACRM consistency increased by incorporating WG, but decreased by incorporating SS. When WG and SS were compounded, the mortar consistency initially rose before falling. The compressive strength of PACRM increased and then decreased as WG was increased. The mechanical properties of PACRM were better enhanced by SS than WG, showing no strength deterioration. The main reason for the improved mechanical properties of polymeric aluminum chloride waste residue in the presence of activators is the increased precipitation of reactive substances, such as C-S-H gels, calcium silica, and $Ca(OH)_2$. The density of the specimens with PACRM and the degree of aggregation of hydration products were significantly enhanced by generating more hydration products in the mortar. Further, the cracks and pores were significantly reduced, and the matrix structure was continuous and dense at 5% SS doping and 3% compound doping.

Keywords: alkali-activated reagents; compressive strength; microstructure; polymeric aluminum chloride residue

1. Introduction

Polymerized aluminum chloride (PAC) is an inorganic, high-efficiency water reducing agent widely used in the wastewater treatment industry (Wei *et al*. 2018, Jia 2018). However, some solid waste residue is generated while producing PAC. With the increasing demand for water purifiers, PAC waste residue also increases, causing severe pollution to the local environment if not effectively treated (Guo *et al*. 2022). Therefore, PAC sludge could be applied recycled. Numerous scholars have conducted in-depth studies on the secondary utilization of industrial slags to effectively utilize them and reduce carbon emissions (Abdulkareem *et al*. 2021, Amer *et al*. 2021a, Rakhimova and Rakhimov 2019). Sulfate excitation is one of the methods used to increase the activity of the waste sludge. Nawaz *et al*. (2020) found that sulfate activation with external fly ash increases the early strength of cement mortar. Ali *et al*. (2021) reported that sulfate activation solves low strength and durability problems of large-volume externally blended fly ash recycled concrete. It is a common practice to improve the activity of slag by alkali excitation and use as cementitious material (Alnahhal *et al*. 2021, Ruengsillapanun *et al*. 2021, Moodi *et al*. 2021, Kilic and Gok 2021). Liu *et al*. (2019) showed that alkali-activated materials perform better than Portland cement. More studies on alkali excitation have been applied to slag activity enhancement (Fang *et al*. 2020, Coppola *et al*. 2020). For instance, Amer *et al*. (2021b) used Na_2SiO_3 and NaOH as excitants to stimulate the activity of slag. They reported that it effectively produced concrete with high compressive strength and desirable compatibility. Chen *et al*. (2021) found that the self-shrinkage of alkali slag cement slurry decreased with increasing alkali content. Earlier, Mohamed (2019) activated a slag with NaOH, Na_2SO_3, and Na_2CO_3 to provide good compressive strength for the concrete. Abdel-Gawwad *et al*. (2019) reported a improvement effect on the activation of slag hydration by mixing concrete waste with slag and using NaOH for alkali excitation.

Alkali excitation improves the activation of slag and steel slag (Sun *et al*. 2020, You *et al*. 2019). Presently, industrial waste materials are reused as construction materials after alkali excitation treatment (Gavali *et al*. 2019). PAC slag primarily contains SiO_2 and Al_2O_3, similar to those of fly ash and slag. Therefore, it is feasible to improve the activity of PAC waste residue by applying activators to cementitious materials. However, few studies have excited the activity of PAC waste residue. The main hindrance here is how to excite PAC slag activity using activators effectively. Although alkali excitation would improve the activity of various industrial wastes, the functional properties of the gelling material would be affected (Tong *et al*. 2021, Marvila *et al*. 2021), probably

*Corresponding author, Ph.D., Professor,
E-mail: xuping@hpu.edu.cn
[a] M.E. Candidate, E-mail: cuiyuhao1214@163.com
[b] Engineer, E-mail: 4026738@qq.com
[c] Professor, E-mail: zhangminxia@126.com
[d] Professor, E-mail: dingyahong@hpu.edu.cn

ISSN: 2287-5301 (Print), 2287-531X (Online)

Table 1 Physical and mechanical properties of Portland cement

Species	Density (g/cm^3)	Specific surface area (m^2/kg)	Setting time (min)		Compressive strength (MPa)		Flexural strength (MPa)	
			Initial set	Final set	Day 3	Day 28	Day 3	Day 28
P.O 42.5	3.1	412	167	233	23	51.6	4.9	7.3

Table 2 Chemical composition of PAC waste residue

Species	SiO_2	Al_2O_3	Fe_2O_3	CaO	MgO	TiO_2	Cl^-	Other
PAC waste residue	45.721	27.80	3.42	5.675	1.34	3.855	2.25	10.389

causing high slurry viscosity and poor flowability (Lu *et al.* 2021). Therefore, it is essential to study the workability of PAC waste slag during alkali excitation.

In this study, PAC waste residue (particle size of 0.075 mm) replaces 15% of cement. After mixing, the flow properties of the mortar were adjusted by external water reducing agent. The activators of the waste slag materials, WG, and SS were added to the cement mortar by single and compound blending. The consistency test, compression test, X-ray diffraction (XRD), and scanning electron microscope (SEM) examined the activator-doped polymeric aluminum chloride residue cement mortar (PACRM) to study the mechanism and effect of the exciter on the PAC waste.

2. Test materials and test design

2.1 Materials

The raw materials include cement, river sand, PAC slag, and polycarboxylic acid water reducing agent. The cement standard is Portland cement of P.O 42.5 from Jiaozuo, Henan Province, China, and the main properties are provided in Table 1. The sand was natural river sand from Jiaozuo, Henan Province, with a grain size of ≤ 4.75 mm. The chloride ions in the PAC waste were removed in advance by Henan Gongyi Xiangji Assembly Component Co., Ltd. from Zhengzhou, Henan Province, China. Its chemical composition is provided in Table 2. The water-reducing agent was ST-01A polycarboxylic acid water reducing agent, produced in Zhengzhou, Henan Province. It is a light yellow liquid with a 30% solid content and 40% water reduction rate. The water used in this study was clean, laboratory tap water.

The results show that the activity of mortar is affected by the single and double mixing of activator (Nasir *et al.* 2020). Water glass (WG) and sodium sulfate (SS), obtained from Jiaozuo City, Henan Province, were used as activators to enhance the activity of PAC waste residue. WG is a white, transparent liquid with a modulus of 3.3, while SS is a white crystalline powder with weak alkaline liquid after water dissolution. The Na_2SO_4 content was > 97%.

2.2 Specimen preparation and testing

To investigate the effect of activator doping amount on

Table 3 Mix proportion of specimen

Codes	Cement (kg/m^3)	PAC waste residue (kg/m^3)	Sand (kg/m^3)	Water (kg/m^3)	Water reducer (%)	WG (%)	SS (%)
B0	382.5	67.5	1350	225			
WG1	382.5	67.5	1350	225	1%	1%	-
WG2	382.5	67.5	1350	225	1%	2%	-
WG3	382.5	67.5	1350	225	1%	3%	-
WG4	382.5	67.5	1350	225	1%	4%	-
WG5	382.5	67.5	1350	225	1%	5%	-
WG6	382.5	67.5	1350	225	1%	6%	-
SS1	382.5	67.5	1350	225	1%	-	1%
SS2	382.5	67.5	1350	225	1%	-	2%
SS3	382.5	67.5	1350	225	1%	-	3%
SS4	382.5	67.5	1350	225	1%	-	4%
SS5	382.5	67.5	1350	225	1%	-	5%
SS6	382.5	67.5	1350	225	1%	-	6%
C1	382.5	67.5	1350	225	1%	1%	1%
C2	382.5	67.5	1350	225	1%	2%	2%
C3	382.5	67.5	1350	225	1%	3%	3%

the activity of PAC waste residue, the specimens were divided into a baseline group and a control group. The base group specimens were expressed as B0. They were made of PAC waste residue (particle size ≤ 0.075 mm) in place of 15% of cement. The control group was made by WG and SS single mixtures and compound blending, respectively. WG1 and SS1 denote specimens containing 1% water glass and 1% sodium sulfate, respectively, while C1 contains 1% water glass and 1% sodium sulfate. The mix proportion of each specimen is given in Table 3.

The specimens for the mechanical test were selected as cubes (dimension of 70.7 × 70.7 × 70.7 mm) according to the Chinese standard JGJ/T70-2009. Each group of cement mortar was tested for consistency after being configured according to the ratio in Table 3. The specimens were subjected to compressive and flexural testing after being placed at 20℃ for 7, 14, and 28 days. Further XRD and SEM tests were performed on each cement pastes under the same matching ratio conditions and after the same maintenance conditions. The obtained results were used to deduce the mechanism of the effect of the exciter on PAC waste slag activity.

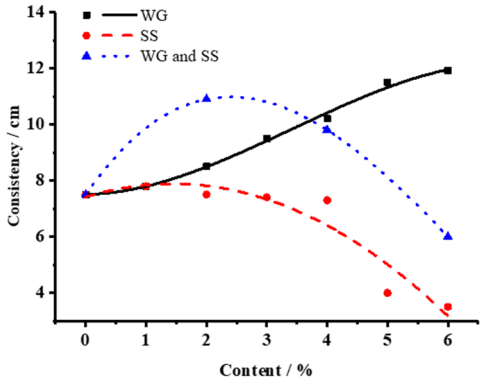

Fig. 1 The trend of mortar consistency with increased activator amount

3. Results and analysis

3.1 Effect of activators on PACRM consistency

The test results of PACRM consistency under various activator admixtures are shown in Fig. 1. The excitant types and mixing methods had different effects on the consistency of cement mortar. By increasing the WG admixture, the mortar consistency increased gradually. The consistency did not differ much from that of the reference group at 1% of the content. The mortar consistency increased almost linearly when the WG admixture was increased. When the mixture reached 6%, the mortar consistency reached 11.9 cm, 58.7% higher than that of the reference group, as the working performance improved. However, the mortar consistency decreased with an increase in sodium sulfate admixture. The effect of the activator on mortar consistency did not vary significantly when the sodium sulfate admixture was between 1% and 3%. The consistency was maintained between 7.3 and 7.8 cm. The mortar consistency value decreased rapidly when the dosage was > 4%. The consistency value at 6% was only 3.5 cm. The main reason is that SS can promote the early mortar setting, and shortening the setting time decreases the mortar consistency rapidly. When the activator was compounded, the mortar consistency value increased first and then dropped. The maximum mortar consistency of 10.9 cm was reached at 1% of WG and SS. Then, it started to decrease with increased dosage, reaching the lowest value of 4.5 cm, lower than the

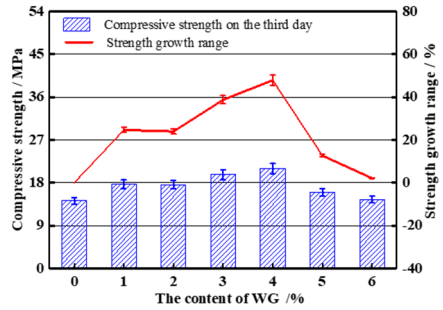

(a) Day 3

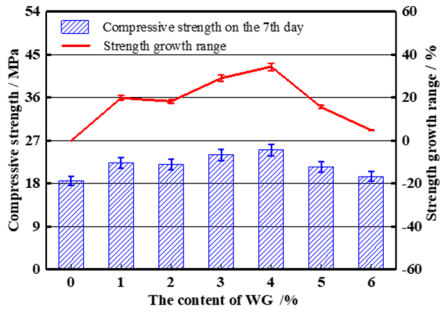

(b) Day 7

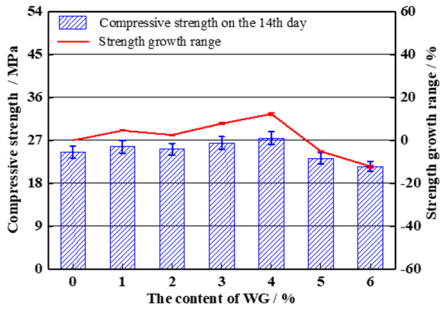

(c) Day 14

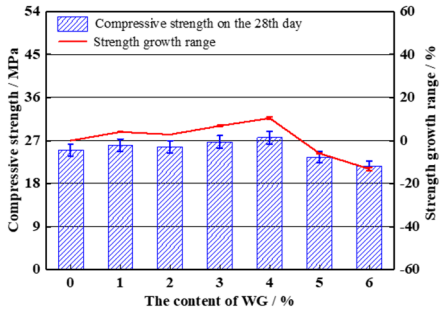

(d) Day 28

Fig. 2 Compressive strength of PACRM specimens mixed with WG

mortar consistency of the B0 group. In summary, PACRM exhibited excellent working performance when the WG single admixture was > 4% or the WG and SS compound admixture was 1%.

3.2 Effect of activator on PACRM compressive strength

Figs. 2(a)-(d) shows the trends of compressive strength and strength growth rate of PACRM specimens with different dosing of WG as an activator at various ages. The growth rate of compressive strength is the ratio of the increment of the compressive strength of each group of specimens over the group B0 to the compressive strength of the group B0. The results are the average of the measured values of the group. The specimens exhibited different strengths at different stages with increased WG admixture proportion in PACRM. The compressive strength of the specimens increased with the activator, i.e., with increased WG dosage from 1% to 4%, where it peaked. The enhancement rate of specimen strength gradually decreases with increasing age, with the largest and mildest change on the 3rd and 28th days, respectively. Therefore, varying the WG dosage significantly affects the early strength of PACRM. At 5% and 6% WG dosages, the compressive strength of the specimens deteriorated on days 3, 7, 14, and 28. The strength improvement rate was lower (or negative) than that of the reference group. As it aged, the strength deteriorated faster, and the loss of compressive strength increased beyond the reference group's value. Thus, the WG dosing was greater than 4%, not conducive to improving the compressive strength of PACRM at the later stage.Figs. 3(a)-(d) shows changes in the compressive strength and strength growth rate of PACRM specimens doped with SS on days 3, 7, 14, and 28. It could be seen that SS better enhanced the mechanical properties of PACRM than WG. We observed that the compressive strength of the specimens at all stages increased with sodium sulfate dosage from 1% to 3%, where the SS3 strength peaked. Meanwhile, as it aged, the strength growth rate of SS1 and SS2 groups decreased gradually, while that of SS3 was steady at a higher level. Moreover, the specimen strength decreased at 4% sodium sulfate admixture, but it was consistently higher than that of the reference group, and the strength growth rate was similar to that of SS1. The compressive strength at all ages peaked at 5% sodium sulfate admixture, with a slight strength depreciation at 6%. However, the decline reduced as aging occurred, probably due to the excess AFt in the mortar. The AFt stability was lower than that of C-S-H. AFt damaged the mortar matrix structure due to the stress generated by its expansion as the age of maintenance grows. Therefore, it is easy to trigger an increase in the number of cracks and a decrease in strength.

$$\begin{cases} \equiv Si-O-Si \equiv +3OH^- \rightarrow [SiO(OH)_3]^- \\ \equiv Si-O-Al \equiv +7OH^- \rightarrow [SiO(OH)_3]^- + [Al(OH)_4]^- \\ 2[Al(OH)_4]^- + 3SO_4^{2-} + 6Ca^{2+} + 4OH^- + 26H_2O \rightarrow 3CaO \cdot Al_2O_3 \cdot 3CaSO_4 \cdot 32H_2O \end{cases} \quad (1)$$

Figs. 4(a)-(d) shows the effect of compound activator on the mechanical properties of PACRM. The specimen strength of PACRM increased with co-activator (SS and WG) dosage. The compressive strength of PAVRM increased with the dosage of each group on the third and

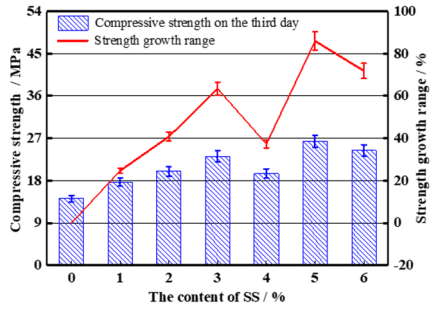

(a) Day 3

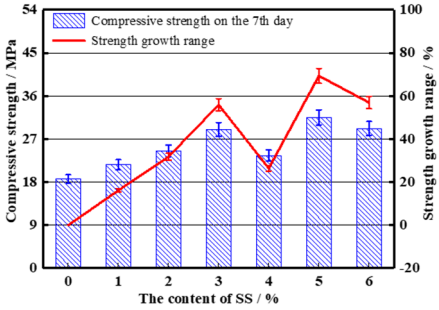

(b) Day 7

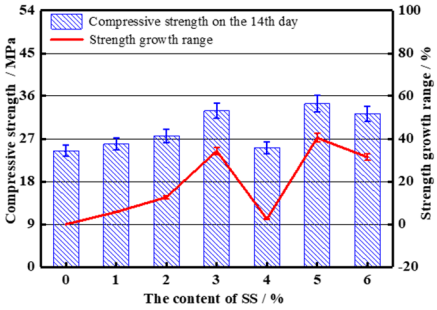

(c) Day 14

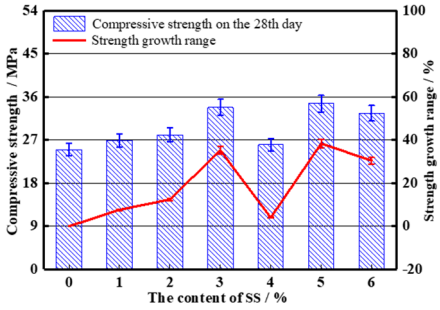

(d) Day 28

Fig. 3 Compressive strength of PACRM specimens mixed with SS

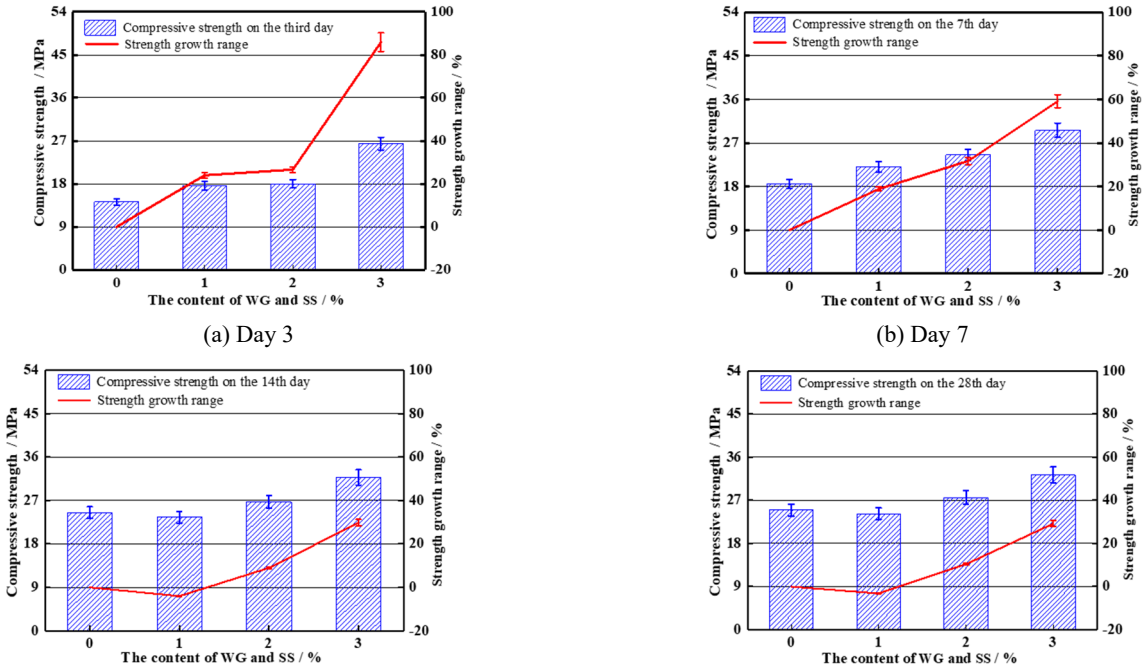

(a) Day 3 (b) Day 7

(c) Day 14 (d) Day 28

Fig. 4 Compressive strength of PACRM specimens compounded with WG and SS

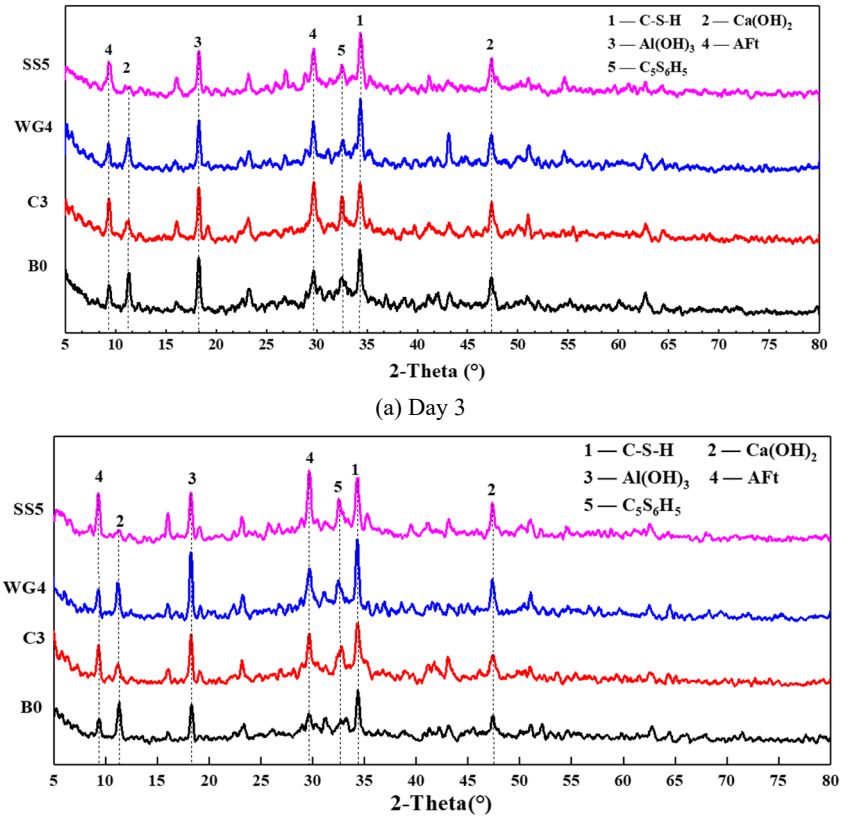

(a) Day 3

(b) Day 28

Fig. 5 XRD analysis results

seventh days, indicating that compounding the activator promoted the early compressive strength of PACRM. Compared to group B0, the strength improvement rate in group C1 decreased by −4.1% and −3.2% on days 14 and 28, respectively. These results suggest a negative effect on the late compressive strength of PACRM when WG and SS

are mixed with 1%, respectively. However, the compressive strength of PACRM increased in C2 and C3 groups on days 14 and 28. The compressive strength and compressive strength growth rate of PACRM peaked at all ages when WG and SS were dosed at 3%, respectively.

3.3 Microstructural analysis

3.3.1 Test analysis of XRD

Four groups of specimens: B0, WG4, SS5, and C3, with the highest compressive strengths of PACRM, were subjected to XRD analysis for their mineral composition. The test result of specimens aged days 3 and 28 are shown in Fig. 5. The abscissa in Fig. 5 indicates the scanning angle of XRD diffraction and the ordinate indicates the intensity. The main hydration products of PACRM are C-S-H, $Ca(OH)_2$, and a large amount of $Al(OH)_3$ at day 3 (Fig. 5(a)). Also, C3, WG4, and SS5 exhibited wave peaks of $Ca(OH)_2$ significantly lower than B0 after mixing with the activator, while the number and height of the C-S-H wave peak significantly increased. We observed that the slurry pH of PAC slag increased to allow the precipitated active substances (SiO_2, Al_2O_3) to react with $Ca(OH)_2$ generated by hydration of Portland cement under the influence of the activator. Therefore, more hydration products were generated, promoting the hydration of the gelling materials in PACRM, thereby improving the mechanical properties. It was also shown in previous literature (Zhao *et al*. 2023, Song *et al*. 2022). Since the covalent bonds of stable glass phases (Si-O-Si, Al-O-Al) in PAC waste residue were broken and transformed into unstable phases (Ma *et al*. 2020), the activity of PAC waste increased (Eq. (1)). As a strong alkaline activator, Na_2SiO_4 accelerates the hydration, generating more C-S-H gels and converting the high sulfur-type hydrated calcium sulfoaluminate to the monosulfur type. This conversion leads to a slight decrease in the material's mechanical strength.

From the XRD test results in Fig. 5(b), the main hydration products in PACRM are AFt and C-S-H gel on day 28. In addition, AFt exhibited a peculiar swelling property, allowing it to fill the pores inside the PACRM specimen and improve the material's mechanical properties. However, too much AFt filling would cause destructive stress via volume expansion, thereby compromising the strength of the specimen. The two hydration products increase with activator incorporation at the early stage. The main reason is that a large amount of $Ca(OH)_2$ is generated after sodium sulfate dosage increases, making micro-cracks inside the mortar; hence, swelling damage occurs. AFt and C-S-H gel can be filled into the micropores of the mortar, thereby improving the structural compactness and strength. The incorporation of sodium sulfate increased the amount of C-S-H, the main hydration product of PACRM, and significantly enhanced the strength of PACRM in the early and late stages.

3.3.2 Test analysis of SEM

The reasons for the variation of the mechanical properties of PACRM can be well responded by the denseness of the microstructure and the microscopic composition at different ages (Zhang *et al*. 2020). The test groups B0, WG1, WG4, WG5, SS1, SS4, SS5, and C3, aged 3 and 28 days, were subjected to SEM tests (Figs. 6-8).

Fig. 6 shows the SEM test results of each group of specimens at day 3. From Fig. 6(a), we observed that the pores in the B0 matrix structure were filled with a minute amount of Aft and C-S-H gels. A small amount of flocculent C-S-H and platelet $Ca(OH)_2$ were also attached to the matrix bulk structure, indicating hydration in progress. By comparing the microscopic morphology of B0 with those of WG1, WG4, and WG5 at the same magnification (Figs. 6(b)-(d)), we found that the number of C-S-H gels increased at WG1, filling the pores. The disappearance of $Ca(OH)_2$, which is smaller in volume, indicates that the incorporation of water glass promoted PACRM hydration. Further, WG4 showed that the surface of PAC slag particles was adhered to by hydration products. A small amount of AFt penetrated through the particles, indicating that PAC slag active material was released as the water glass doping increased. More AFt was generated on the surface of the PAC slag particles in WG5. It completely wrapped the surface of the particles after increasing the water glass dosing. It prevents the subsequent precipitation of active material in PAC slag, unconducive to strength development. Figs. 6(e)-(g) illustrate that the hydration products of SS1 are C-S-H gels and $Ca(OH)_2$ attached to the matrix compared with group B0. The number of fibrous gels in SS4 and SS5 increased and filled the pores of the matrix. Meanwhile, a higher number of C-S-H gels and AFt wrapped around the PAC slag particles were found in SS5, indicating that the activity of the PAC slag material was enhanced by sodium sulfate, improving the mechanical properties. Moreover, numerous tiny pieces of $Ca(OH)_2$ appeared in C3 (Fig. 6(h)). These $Ca(OH)_2$ specs were attached to numerous C-S-H gels, resulting in no pores and cracks in the matrix structure, and the material's mechanical properties are optimized.

Fig. 7 shows the microstructure of each group of specimens observed at 300x magnification on day 28. As shown in Figs. 7(a) and 8(a), the matrix structure of group B0 was loose and porous, with C-S-H gels filling the pores. The bulk hydration product is $Ca(OH)_2$. WG1 and WG4 exhibited improved densities than WG5 at the same multiplicity Figs. 7(b)-(d). Also, more cracks in WG5 were observed, accounting for the depreciated mechanical properties of PACRM. As shown in Figs. 8(b)-(d), the hydration products wrapped the mortar matrix well. However, more microcracks appeared in the matrix structure of WG5 as Na_2SiO_4 doping increased. The hydration products of WG5 were significantly more than those of WG1. The microcrack interior in the WG5 group was filled with C-S-H gel and Aft, different from the microcracks of WG1. There were cracks on the surface of the matrix, attributed to stress damage caused by volume expansion of AFt in the matrix. On the other hand, the WG4 group was microscopically dense and did not produce significant microcracks which was also why the compressive strength of PACRM peaked when the water glass was dosed with 4% and decreased by 5%.

From Figs. 7(e)-(g), we found that the denseness of the

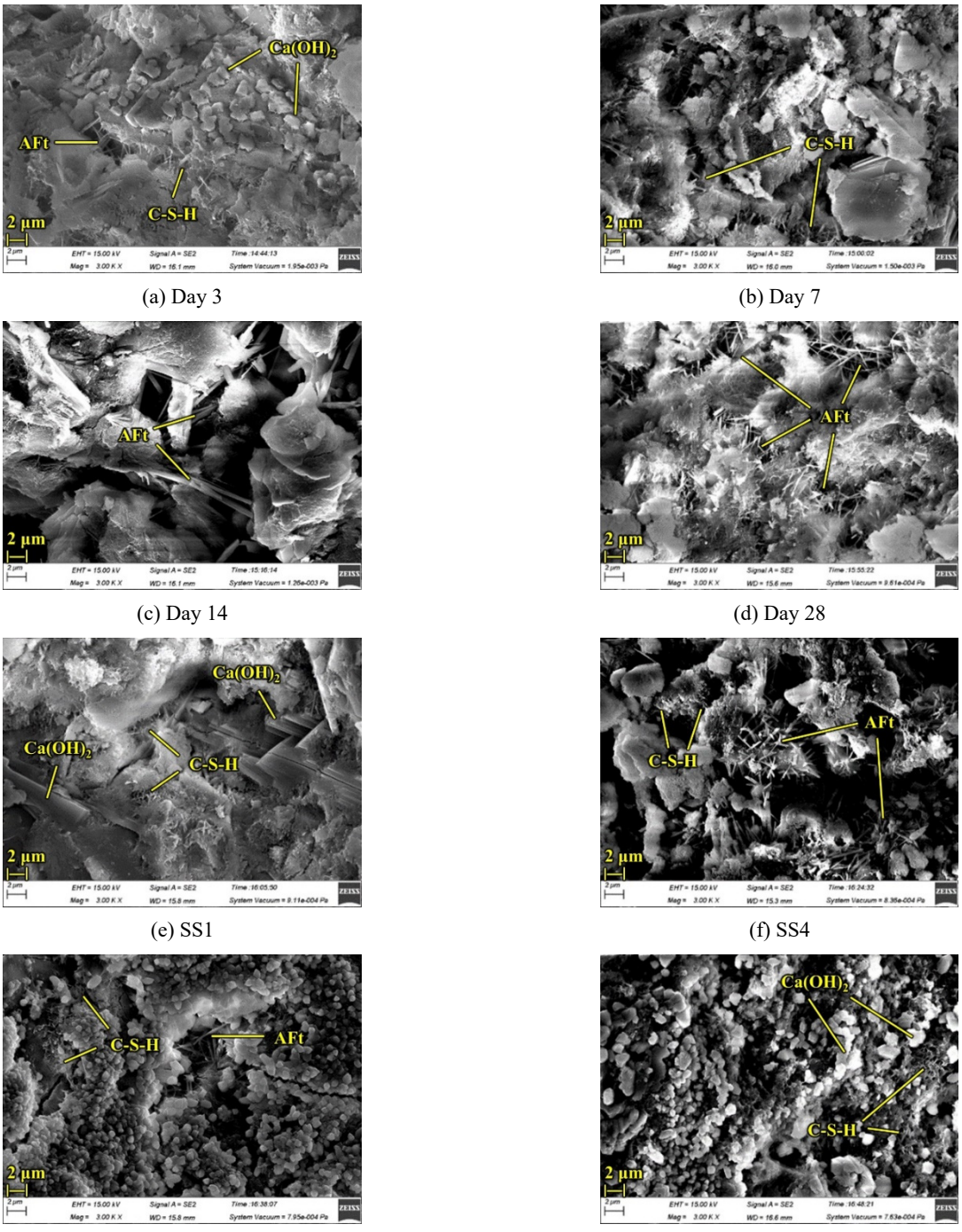

(a) Day 3 (b) Day 7

(c) Day 14 (d) Day 28

(e) SS1 (f) SS4

(g) SS5 (h) C3

Fig. 6 SEM testing of specimens aged on day 3

mortar matrix structure gradually increases with sodium sulfate dosage. No cracks or holes were observed in the matrix at 5% doping. From Figs. 8(e)-(g), small pieces of $Ca(OH)_2$ were scattered in the SS1 group, with a lower degree of aggregation of hydration products. Wide microcracks in the mortar matrix were still evident, indicating that the activator dosing was too low, leading to a poor excitation effect. The degree of aggregation of hydration products in SS4 and SS5 groups was better after increasing the activator dosage. The PAC slag in the SS4 group was well wrapped by the hydration products, with no noticeable scattered PAC slag particles. Only a relatively small number of microcracks appeared. Also, the crack width reduced significantly, maintaining a better bond. The matrix surface of the SS5 group exhibited some unaggregated $Ca(OH)_2$, and there were still many AFt connections and filling between the particles and in the internal pores. These occurrences indicate that under the excitation of 5% sodium sulfate, the hydration products of PAC waste and cement crystallized adequately to form a continuous and dense whole. We opine this was the main reason why the mechanical properties of PACRM improved

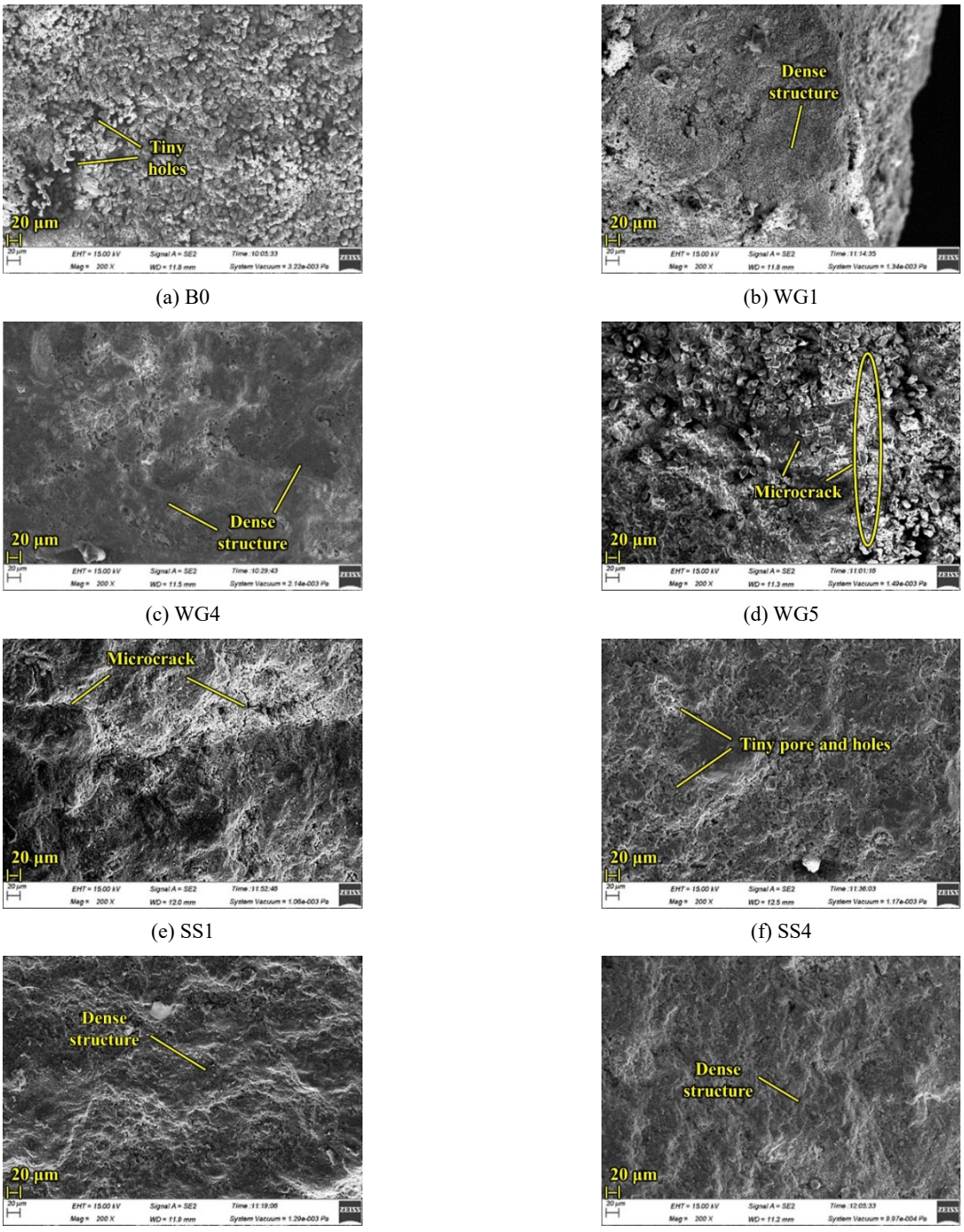

Fig. 7 SEM testing of specimens aged 28 days at 300 magnification

at 5% dosing. As shown in Figs. 7(h) and 8(h), the C3 group was denser than the B0 group (without microfractures). Therefore, a large amount of C-S-H gel and AFt generated in the C3 group sufficed, exhibiting a good filling effect on the microfractures, thus enhancing the compressive strength of PACRM.

4. Conclusions

This study investigated the consistency, mechanical properties, and microscopic composition of PACRM (with different activators and different doping amounts). The conclusions are shown as follows.

- The mortar consistency of PACRM was increased by WG. The property was reduced after adding SS. The mortar consistency dropped abruptly when the admixture amount was > 4%. And when the activator

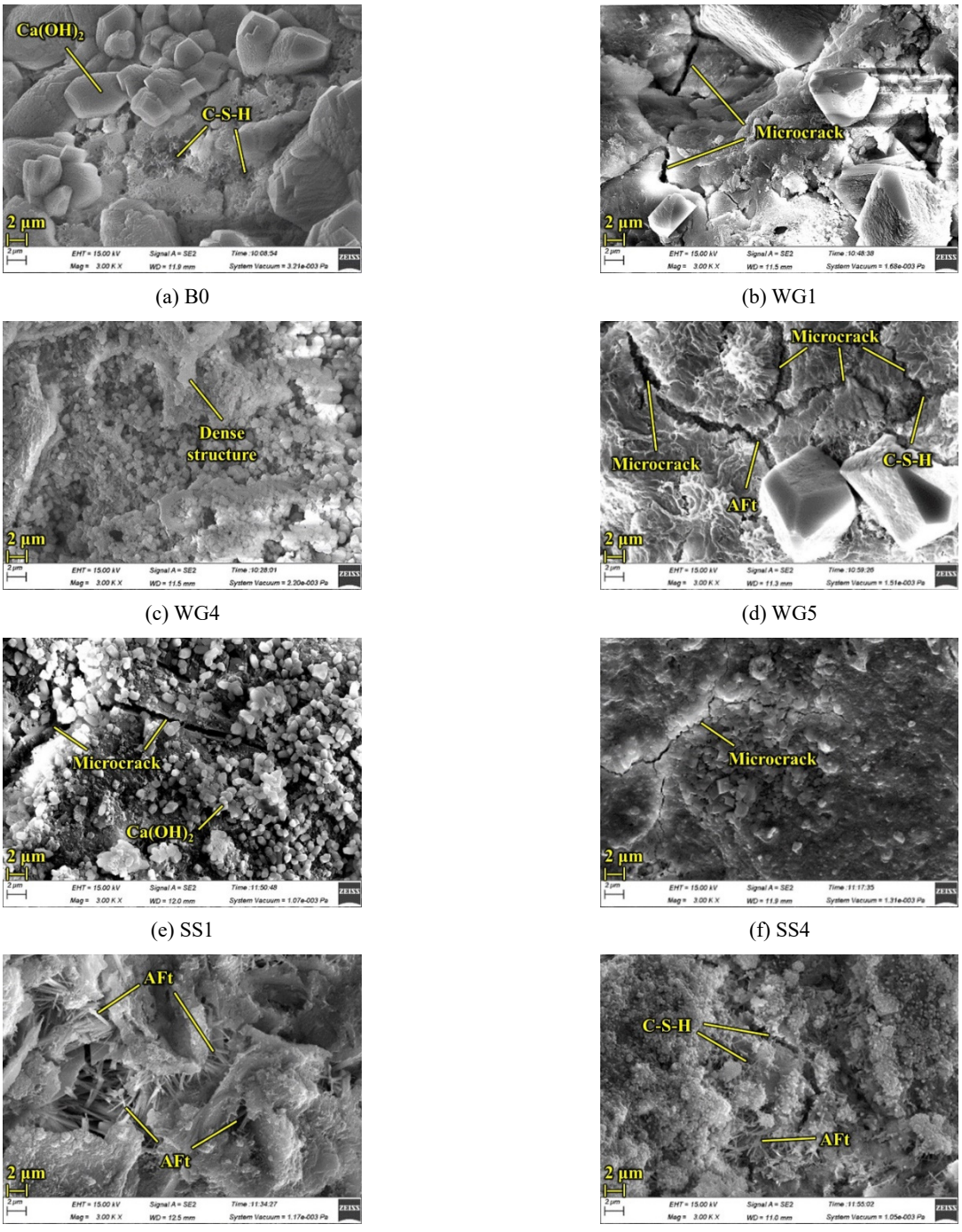

Fig. 8 SEM testing of specimens aged on day 28 at 3000 magnification

was compounded, the mortar consistency rose at first before dropping. PACRM has good working performance when the single admixture of WG is > 4% or the compound admixture of WG and SS is 1%.

- The compressive strength of PACRM rose initially before dropping as WG dosage increased. When the doping amount was > 4%, it became unconducive to improve the compressive strength of PACRM. Generally, SS better enhanced the mechanical properties of PACRM than WG. It peaked at 5% of SS alone or compounded 3% of SS and WG.
- The main reason for the increased activity of PAC waste residue in the presence of an activator is the increased precipitation of active substances. Therefore, more hydration products (such as C-S-H gel, Aft, and $Ca(OH)_2$) were generated in the mortar system. The denseness of PACRM improved significantly by filling numerous hydration products at 5% SS dosage and 3% compounding. As a result, the number of cracks and pores reduced considerably, and the matrix structure became

appreciably continuous and dense.

Acknowledgments

Financial supports from the Key Science and Technology Program of Henan Province, China (No. 202102310253), the Youth Key Teacher Project of Henan Provincial Colleges and Universities (2017GGJS054), Joint Funds of the National Natural Science Foundation of China (No. U1904188), the Doctor Foundation of Henan Polytechnic University (No. B2016-67), and the Science and Technology Project of Henan Provincial Department of Transportation, China (No. 2019J-2-13) are gratefully appreciated. Some or all data, models, or code that support the findings of this study are available from the corresponding author upon reasonable request. All data, models, and code generated or used during the study appear in the submitted article.

References

Abdel-Gawwad, H.A., Rashad, A.M. and Heikal, M. (2019), "Sustainable utilization of pretreated concrete waste in the production of one-part alkali-activated cement", *J. Clean. Prod.*, **232**, 318-328. https://doi.org/10.1016/j.jclepro.2019.05.356

Abdulkareem, M., Havukainen, J., Nuortila-Jokinen, J. and Horttanainen, M. (2021), "Environmental and economic perspective of waste-derived activators on alkali-activated mortars", *J. Clean. Prod.*, **280**, 124651. https://doi.org/10.1016/j.jclepro.2020.124651

Ali, B., Gulzar, M.A. and Raza, A. (2021), "Effect of sulfate activation of fly ash on mechanical and durability properties of recycled aggregate concrete", *Constr. Build. Mater.*, **277**, 122329. https://doi.org/10.1016/j.conbuildmat.2021.122329

Alnahhal, M.F., Kim, T. and Hajimohammadi, A. (2021), "Waste-derived activators for alkali-activated materials: A review", *Cem. Concr. Compos.*, **118**, 103980. https://doi.org/10.1016/j.cemconcomp.2021.103980

Amer, I., Kohail, M., El-Feky, M.S., Rashad, A. and Khalaf, M.A. (2021a), "A review on alkali-activated slag concrete", *Ain Shams Eng. J.*, **12**(2), 1475-1499. https://doi.org/10.1016/j.asej.2020.12.003

Amer, I., Kohail, M., El-Feky, M.S., Rashad, A. and Khalaf, M.A. (2021b), "Characterization of alkali-activated hybrid slag/cement concrete", *Ain Shams Eng. J.*, **12**(1), 135-144. https://doi.org/10.1016/j.asej.2020.08.003

Chen, W., Li, B., Wang, J. and Thom, N. (2021), "Effects of alkali dosage and silicate modulus on autogenous shrinkage of alkali-activated slag cement paste", *Cem. Concr. Res.*, **141**, 106322. https://doi.org/10.1016/j.cemconres.2020.106322

Coppola, L., Coffetti, D., Crotti, E., Gazzaniga, G. and Pastore, T. (2020), "The durability of one-part alkali-activated slag-based mortars in different environments", *Sustainability*, **12**(9), 3561. https://doi.org/10.3390/su12093561

Fang, S., Lam, E.S.S., Li, B. and Wu, B. (2020), "Effect of alkali contents, moduli and curing time on engineering properties of alkali activated slag", *Constr. Build. Mater.*, **249**, 118799. https://doi.org/10.1016/j.conbuildmat.2020.118799

Jia, R. (2018), "Experimental Research on Removal of Turbidity and UV254 by Poly-aluminum Chloride (PAC)", *E3S Web of Conferences*, **53**(3), 04006. https://doi.org/10.1051/e3sconf/20185304006

Kilic, I. and Gok, S.G. (2021), "A study on investigating the properties of alkali-activated roller compacted concretes", *Adv. Concrete Constr., Int. J.*, **12**(2), 117-123. https://doi.org/10.12989/acc.2021.12.2.117

Gavali, H.R., Bras, A., Faria, P. and Ralegaonkar, R.V. (2019), "Development of sustainable alkali-activated bricks using industrial wastes", *Constr. Build. Mater.*, **215**, 180-191. https://doi.org/10.1016/j.conbuildmat.2019.04.152

Guo, J., Zhou, Z., Ming, Q., Huang, Z., Zhu, J., Zhang, S., Xu, J., Xi, J., Zhao, Q. and Zhao, X. (2022), "Recovering precipitates from dechlorination process of saline wastewater as poly aluminum chloride", *Chem. Eng. J.*, **427**, 131612. https://doi.org/10.1016/j.cej.2021.131612

Liu, Y., Shi, C., Zhang, Z. and Li, N. (2019), "An overview on the reuse of waste glasses in alkali-activated materials", *Resour. Conserv. Recy.*, **144**, 297-309. https://doi.org/10.1016/j.resconrec.2019.02.007

Lu, C., Zhang, Z., Shi, C., Li, N., Jiao, D. and Yuan, Q. (2021), "Rheology of alkali-activated materials: A review", *Cem. Concr. Compos.*, **121**, 104061. https://doi.org/10.1016/j.cemconcomp.2021.104061

Ma, C., Zhao, B., Wang, L., Long, G. and Xie, Y. (2020), "Clean and low-alkalinity one-part geopolymeric cement: effects of sodium sulfate on microstructure and properties", *J. Clean. Prod.*, **252**, 119279. https://doi.org/10.1016/j.jclepro.2019.119279

Marvila, M.T., Azevedo, A.R.G.D., Matos, P.R.D., Monteiro, S.N. and Vieira, C.M.F. (2021), "Rheological and the fresh state properties of alkali-activated mortars by blast furnace slag", *Mater.*, **14**(8), 2069. https://doi.org/10.3390/ma14082069

Mohamed, O.A. (2019), "A review of durability and strength characteristics of alkali-activated slag concrete", *Mater.*, **12**(8), 1198. https://doi.org/10.3390/ma12081198

Moodi, F., Norouzi, S. and Dashti, P. (2021), "Mechanical properties and durability of alkali-activated slag repair mortars containing silica fume against freeze-thaw cycles and salt scaling attack", *Adv. Concrete Constr., Int. J.*, **11**(6), 493-505. https://doi.org/10.12989/acc.2021.11.6.493

Nawaz, M.A., Ali, B., Qureshi, L.A., Aslam, H.M.U., Hussain, I., Masood, B. and Raza, S.S. (2020), "Effect of sulfate activator on mechanical and durability properties of concrete incorporating low calcium fly ash", *Case Stud. Constr. Mater.*, **13**, e407. https://doi.org/10.1016/j.cscm.2020.e00407

Nasir, M., Johari, M.A.M., Yusuf, M.O., Maslehuddin, M. and Al-Harthi, M.A. (2020), "Effect of alkaline activators on the fresh properties and strength of silico-manganese fume-slag activated mortar", *Adv. Concrete Constr., Int. J.*, **10**(5), 403-416. https://doi.org/10.12989/acc.2020.10.5.403

Rakhimova, N.R. and Rakhimov, R.Z. (2019), "Reaction products, structure and properties of alkali-activated metakaolin cements incorporated with supplementary materials–a review", *J. Mater. Sci. Technol.*, **8**(1), 1522-1531. https://doi.org/10.1016/j.jmrt.2018.07.006

Ruengsillapanun, K., Udtaranakron, T., Pulngern, T., Tangchirapat, W. and Jaturapitakkul, C. (2021), "Mechanical properties, shrinkage, and heat evolution of alkali activated fly ash concrete", *Constr. Build. Mater.*, **299**, 123954. https://doi.org/10.1016/j.conbuildmat.2021.123954

Song, Q., Guo, M.Z. and Ling, T.C. (2022), "A review of elevated-temperature properties of alternative binders: Supplementary cementitious materials and alkali-activated materials", *Constr. Build. Mater.*, **341**, 127894. https://doi.org/10.1016/j.conbuildmat.2022.127894

Sun, J., Zhang, Z., Zhuang, S. and He, W. (2020), "Hydration properties and microstructure characteristics of alkali–activated steel slag", *Constr. Build. Mater.*, **241**, 118141. https://doi.org/10.1016/j.conbuildmat.2020.118141

Tong, S., Yuqi, Z. and Qiang, W. (2021), "Recent advances in

chemical admixtures for improving the workability of alkali-activated slag-based material systems", *Constr. Build. Mater.*, **272**, 121647. https://doi.org/10.1016/j.conbuildmat.2020.121647

Wei, H., Gao, B., Ren, J., Li, A. and Yang, H. (2018), "Coagulation/flocculation in dewatering of sludge: a review", *Water Res.*, **143**, 608-631. https://doi.org/10.1016/j.watres.2018.07.029

You, N., Li, B., Cao, R., Shi, J., Chen, C. and Zhang, Y. (2019), "The influence of steel slag and ferronickel slag on the properties of alkali-activated slag mortar", *Constr. Build. Mater.*, **227**, 116614. https://doi.org/10.1016/j.conbuildmat.2019.07.340

Zhang, Q., Ji, T., Yang, Z., Wang, C. and Wu, H. (2020), "Influence of different activators on microstructure and strength of alkali-activated nickel slag cementitious materials", *Constr. Build. Mater.*, **235**, 117449. https://doi.org/10.1016/j.jclepro.2022.135547

Zhao, Q., Ma, C., Huang, B. and Lu, X. (2023), "Development of alkali activated cementitious material from sewage sludge ash: Two-part and one-part geopolymer", *J. Clean. Prod.*, **384**, 135547. https://doi.org/10.1016/j.jclepro.2022.135547